

Title: A Revised Method of Presenting Wavenumber-Frequency Power Spectrum Diagrams That Reveals the Asymmetric Nature of Tropical Large-scale Waves

Authors: Winston C. Chao (NASA/GSFC), Bo Yang and Xiouhua Fu (International Pacific Research Center, University of Hawaii at Manoa)

Journal: Journal of Climate (submitted)

Popular Summary

The popular method of presenting wavenumber-frequency power spectrum diagrams for studying tropical large-scale waves in the literature is shown to give an incomplete presentation of these waves. The so-called "convectively-coupled Kelvin (mixed Rossby-gravity) waves" are presented as existing only in the symmetric (anti-symmetric)--with respect to the equator--component of the diagrams. This is obviously not consistent with the published composite/regression studies of "convectively-coupled Kelvin waves," which illustrate the asymmetric nature--composed of both symmetric and anti-symmetric components--of these waves. The cause of this inconsistency is revealed in this note and a revised method of presenting the power spectrum diagrams is proposed. When this revised method is used, "convectively-coupled Kelvin waves" do show anti-symmetric components, and "convectively-coupled mixed Rossby-gravity waves (also known as Yanai waves)" do show a hint of symmetric components. These results bolster a published proposal that these waves be called "chimeric Kelvin waves," "chimeric mixed Rossby-gravity waves," etc. This revised method of presenting power spectrum diagrams offers a more rigorous means of comparing the GCM output with observations by calling attention to the capability of GCMs in correctly simulating the asymmetric characteristics of the equatorial waves.

--

**A Revised Method of Presenting Wavenumber-Frequency Power Spectrum
Diagrams That Reveals the Asymmetric Nature of Tropical Large-scale Waves**

Winston C. Chao

Laboratory for Atmospheres, NASA/Goddard Space Flight Center
Greenbelt, MD 20771

Bo Yang and Xiouhua Fu

International Pacific Research Center
School of Ocean and Earth Science and Technology
University of Hawaii at Manoa
Honolulu, HI 96822

(To be submitted to J. Climate, November 2007)

Corresponding Author Address:
Dr. Winston C. Chao
Code 613.2
NASA/Goddard Space Flight Center
Greenbelt, MD 20771
Winston.c.chao@nasa.gov

Abstract

The popular method of presenting wavenumber-frequency power spectrum diagrams for studying tropical large-scale waves in the literature is shown to give an incomplete presentation of these waves. The so-called “convectively-coupled Kelvin (mixed Rossby-gravity) waves” are presented as existing only in the symmetric (anti-symmetric) component of the diagrams. This is obviously not consistent with the published composite/regression studies of “convectively-coupled Kelvin waves,” which illustrate the asymmetric nature of these waves. The cause of this inconsistency is revealed in this note and a revised method of presenting the power spectrum diagrams is proposed. When this revised method is used, “convectively-coupled Kelvin waves” do show anti-symmetric components, and “convectively-coupled mixed Rossby-gravity waves (also known as Yanai waves)” do show a hint of symmetric components. These results bolster a published proposal that these waves be called “chimeric Kelvin waves,” “chimeric mixed Rossby-gravity waves,” etc. This revised method of presenting power spectrum diagrams offers a more rigorous means of comparing the GCM output with observations by calling attention to the capability of GCMs in correctly simulating the asymmetric characteristics of the equatorial waves.

1. Introduction

Tropical large-scale waves, both observed and modeled, have been analyzed by the power spectrum analysis method and presented in the form of wavenumber-frequency power spectrum diagrams (e.g., Hayashi 1982, Takayabu 1994). To make the tropical waves stand out in these diagrams, Wheeler and Kiladis (1999; hereafter WK) constructed a background power spectrum (their Fig. 2) by averaging the “raw” power spectra of the symmetric (with respect to the equator) and anti-symmetric components (their Fig. 1) and then applying, many times, a 1-2-1 smoothing filter in both frequency and wavenumber domains. For both symmetric and anti-symmetric components, the ratio of the “raw” power spectrum to the same background power spectrum is then presented as the final spectrum (their Fig. 3). The WK method of presenting wavenumber-frequency power spectrum diagrams has become popular among researchers who compare GCM model output with observations (e.g., Lin et al. 2006). However, despite its popularity, this method can be improved upon.

In their Fig 3, what WK identified as “convectively-coupled Kelvin waves” are seen only in the symmetric component of the diagrams, and what WK identified as “convectively-coupled mixed Rossby-gravity waves” (also known as Yanai waves) are seen only in the anti-symmetric component of the diagrams. However, in the composite/regression analysis of “convectively-coupled Kelvin waves” by Straub and Kiladis (2002, their Fig. 16), these waves are clearly not symmetric with respect to the equator, and thus should have both symmetric and anti-symmetric components. This asymmetry is obvious from the fact that these waves are associated with oscillations

within ITCZs, and ITCZs are rarely symmetric with respect to the equator. In fact, if one examines Fig. 1 of WK, the “raw” power spectra, closely; it is discernable that in the anti-symmetric component there is a local peak around frequency 0.22 cpd (cycles per day) and eastward wavenumbers 6 and 7 (this spot in the diagram is hereafter referred to as the F0.22E6-7 spot), corresponding to the “convectively-coupled Kelvin waves.” This note reveals the reason why Fig. 3 of WK does not show the asymmetric nature of the equatorial waves, and offers a revised method of presenting the power spectra. It also provides the wavenumber-frequency spectral diagrams constructed with our revised method. This note is concluded with some implications of our findings.

2. The cause of the discrepancy and a solution

The cause of the above-mentioned discrepancy lies in the way that the background power spectrum is constructed. When constructing the background power spectrum, WK averaged of the “raw” power spectra of the symmetric and anti-symmetric components and applied a smoothing filter many times to the average to obtain a single background power spectrum (the 10-based logarithm of it is shown in Fig. 2 of WK). WK then used the same background power spectrum for both symmetric and anti-symmetric components when they divided the “raw” power spectra of these components (the 10-based logarithm of them are shown in Fig. 1 of WK) by the background power spectrum to obtain their final spectral diagrams (Fig. 3 of WK) for the two components. This has obscured the anti-symmetric component of “convectively-coupled Kelvin waves.” For example, the local weak peak in the “raw” anti-symmetric diagram (Fig. 1a

of WK) at F0.22E6-7 was divided by a large background, which has a large contribution from the symmetric component, and therefore it is not seen as a peak at all in the resulting ratio, as presented in Fig. 3a of WK.

The solution to this discrepancy is to revise the method of constructing the background in two steps. One is to use separate background spectra for the symmetric and anti-symmetric components. For each component, the background will be constructed from filtering its own “raw” power spectrum. The other step is, instead of filtering the “raw” power spectrum of each component, to filter the 10-based logarithm of the “raw” power spectrum of each component many times and then to take the 10-based exponential to get each background. The first step is necessary because the intent of constructing the background is to use it to compare with (i.e., either to subtract from and to divide) the “raw” power to make the local peaks in the “raw” spectrum stand out. Thus, it is more logical to use the symmetric and anti-symmetric components separately to construct the background for each component. The second step is necessary because the “raw” power spectrum has, in most of the wavenumber-frequency domain, exponential-like distribution in both the frequency and the wavenumber directions (which is the reason 10-based logarithm is used in WK’s Figs. 1 and 2) and the 1-2-1 filter applied to the “raw” power spectrum tends to create a false increase in the magnitude of the background power spectrum. In essence, when a 1-2-1 filter is applied to an exponential function, it increases the value of the exponential function. The new figure, which corresponds to WK’s Figure 3, presents, for each of the symmetric and anti-symmetric components, the ratio of the “raw” spectrum to its new background.

3. The spectral diagrams obtained with the revised method

We revised WK's computer code, provided by M. Wheeler, according to our two-step revision. We used the daily outgoing longwave radiation (OLR) dataset of Liebmann and Smith (1996) from 1982 to 1991. The data resolution was 2.5° latitude by 2.5° longitude; data from 15°S to 15°N were used. The results, corresponding to Fig. 3 of WK (i.e., the ratio between the "raw" power and the new background), are shown in Fig. 1. The corresponding power spectrum diagrams without our revision are given in Fig. 2 for comparison purpose. Two whited-out rectangular areas on the right side of the diagrams are not plotted; the reason for this was given on page 377 of WK. Fig. 2 does not match WK's Fig. 3 exactly. This may be due to the different way of data handling prior to the use of the WK code. Also, WK's used a data period of 16.5 years (vs. our 10 years) and their data were twice-daily (vs. our daily data). However, Fig. 2 is generally consistent with WK's Fig. 3. The peak values for "convectively-coupled Kelvin waves" and "mixed Rossby-gravity waves" are lower in Fig. 1 than in Fig. 2. This is the result of the fact that in the peak regions in Fig. 2 the background is lower than those computed with our method.

Consistent with what we discussed before, Fig. 1a shows that the "convectively-coupled Kelvin waves" now also have anti-symmetric components as indicated by the peak at the F0.22E6-7 spot. This peak has a magnitude slightly above 1.1 (i.e., the "raw" power being 10 percent above the background), a level considered by WK as statistically significant. Since at the peak regions of the diagrams our backgrounds have higher values than that from the WK method, a value greater than 1.1 in our diagrams is more

statistically significant than the same value using the WK method. The special dotted contour line of a value of 1.05 surrounding the F0.22E6-7 peak indicates that this peak region is aligned with the same Kelvin wave dispersion line of 25 m equivalent depth, which is shown as a dashed straight line, as the symmetric “convectively-coupled Kelvin waves” are. This alignment becomes even clearer when northern summer data only are used, as discussed in the next paragraph. Thus, this peak region is a reflection of the anti-symmetric component of the “convectively-coupled Kelvin waves.” This peak in Fig. 1a is completely missing in Fig. 2a. The “convectively-coupled mixed Rossby-gravity waves” now also have a hint of symmetric components as indicated by the weak peak at F0.29E0, which lies close to the dispersion curve of the mixed Rossby-gravity wave of 25 m equivalent depth (the dashed curve in Fig. 1b). Also noteworthy is that the anti-symmetric components of both the “convectively-coupled equatorial Rossby waves” and the MJO are stronger in Fig. 1a than in Fig. 2a. The peak at F0.26W5 in Fig. 1a, easily seen in Fig. 2a as well, is curious. This peak exists in WK’s Fig. 3a also, but is shifted slightly to westward wavenumber 6. Unlike the peak at F0.22E6-7, it does not have a counterpart in the symmetric diagram, Fig. 1b.

When Fig. 1 is redone with data of the Jun-Jul-Aug season only (i.e., only the 96-day segments with mid-date in the JJA season are used), the results (Fig. 3a) show that the anti-symmetric component has much stronger values in the region covering the F0.22E6-7 spot. This shaded region with values greater than 1.1 has an orientation following the Kelvin waves normal mode line corresponding to an equivalent depth of about 25 m in Fig. 3b). Therefore, this region is a distinct counterpart to the “convectively-coupled Kelvin waves” in the symmetric diagram (Fig. 3b), a reflection of

the existence of the anti-symmetric component of the “convectively-coupled Kelvin waves” (which is the most significant result of our study.) This is consistent with the fact that ITCZs are more asymmetric in the JJA season. In the symmetric component the minor peak at the F0.29E0 spot exists in the JJA season, with a peak value just over 1.1, but is shifted slightly toward eastward wavenumber 1 in the DJF season (Figs. 3b and 4b). Notice that for either anti-symmetric or symmetric component the backgrounds for the two seasons are not the same; one need keep this in mind when comparing Fig. 3 and Fig. 4. The anti-symmetric peak at F0.26W5 is easily recognized in the DJF season, but is barely discernable in the JJA season.

4. Implications

The above outcome suggests that the term “convectively-coupled Kelvin waves” is inappropriate. This is because the term “Kelvin waves” has the connotation of being symmetric and having no meridional wind components. Chao (2007) has proposed that a better descriptor for “convectively-coupled Kelvin waves” is chimeric Kelvin waves, based on the fact that even in a symmetric “convectively-coupled Kelvin wave” there is a sizeable Rossby-wave component. The point made in this note further bolsters the use of the term chimeric Kelvin waves and the other similar terms: chimeric Rossby waves and chimeric mixed Rossby-gravity waves. Together these waves may be called chimeric equatorial waves. The adjective chimeric means “composed of parts of different origin.” The observed “convectively-coupled Kelvin waves,” being asymmetric, contain not only Kelvin waves and Rossby waves but also mixed Rossby-gravity waves. Thus, chimeric

Kelvin wave is a better descriptor. The name Kelvin is retained to acknowledge the fact that these waves are eastward moving. The modifier “convectively-coupled” can be omitted for the sake of brevity.

Similar to what Takayabu (1994) did, WK compared, in their Fig. 3, the outgoing longwave radiation (OLR) spectra with the dispersion curves for linear normal modes of the shallow water equation on an equatorial β -plane and found a close match for an equivalent depth of about 25 m for chimeric Kelvin waves and chimeric mixed Rossby-gravity waves. There have been attempts to explain this match (e.g., Lindzen 2003), but a well-accepted explanation is still elusive. Our pointing out the fact that chimeric Kelvin waves and chimeric mixed Rossby-gravity waves have anti-symmetric and symmetric components, respectively, has added another dimension to this puzzling match: i.e., both symmetric and anti-symmetric components of chimeric Kelvin waves exhibit the property of matching with linear normal Kelvin modes, which are symmetric. Although we are not yet prepared to make a similar statement about chimeric mixed Rossby-gravity waves, the fact that the peak at F0.29E0 in the symmetric component in Fig. 3b lies very close to the dispersion curve for mixed Rossby-gravity waves corresponding to an equivalent depth of 25 m--which is the same equivalent depth as for chimeric Kelvin waves--is very intriguing.

The significance of pointing out the above findings is that in the attempt to explain the origin of tropical large-scale waves, it is helpful to have a deeper insight into the observed properties of these waves. Also, our revised method of presenting the spectral diagrams of chimeric equatorial waves offers a more rigorous means of comparing the GCM output with observations by calling attention to the capability of the

GCMs to correctly simulate the asymmetric characteristics of these waves (i.e., their capability to correctly simulate the peak at $F0.22E6-7$ in the anti-symmetric diagram, Fig. 1a, and the corresponding region in Fig. 3a.)

Acknowledgments. Winston Chao was supported by the Modeling, Analysis and Prediction program of NASA Science Mission Directorate. Bo Yang and Xiouhua Fu were supported by NASA Earth Science Program, NSF Climate Dynamics Program, and IPRC. IPRC is sponsored by NASA, NOAA, and the Japan Agency for Marine-Earth Science and Technology (JAMSTEC). Matthew Wheeler provided the WK code for the wavenumber-frequency diagram. Myong-In Lee, Phil Pegion, and Baode Chen of NASA/Goddard/GMAO provided their versions of the WK code for reference purposes. The OLR data used were from Liebmann and Smith of NOAA/CDC.

References

- Chao, W. C., 2007: Chimeric equatorial waves as a better descriptor for “convectively-coupled equatorial waves”. *J. Meteor. Soc. Japan*, **85**, 521-524.
- Hayashi, Y., 1982: Space-time spectral analysis and its applications to atmospheric waves. *J. Meteor. Soc. Japan*, **60**, 156-171.
- Lin, J.-L., et al., 2006: Tropical intraseasonal variability in 14 IPCC AR4 climate models. Part I: Convective signals. *J. Climate*, **19**, 2665-2690.
- Liebmann, B., and C. A. Smith, 1996: Description of a complete (interpolated) outgoing longwave radiation dataset. *Bull. Amer. Meteor. Soc.*, **77**, 1275-1277.
- Lindzen, R. S., 2003: The interaction of waves and convection in the tropics. *J. Atmos. Sci.*, **60**, 3009-3020.
- Straub, K. H., and G. N. Kiladis, 2002: Observations of a convectively-coupled Kelvin wave in the eastern Pacific ITCZ. *J. Atmos. Sci.*, **59**, 30–53.
- Takayabu, Y. N., 1994: Large-scale cloud disturbances associated with equatorial waves. Part I.: Spectral features of the cloud disturbances. *J. Meteor. Soc. Japan*, **72**, 433-448.
- Wheeler, M. C., and G. N. Kiladis, 1999: Convectively-coupled equatorial waves: Analysis of clouds and temperature in the wave-number-frequency domain. *J. Atmos. Sci.*, **56**, 374-399.

Figure Captions

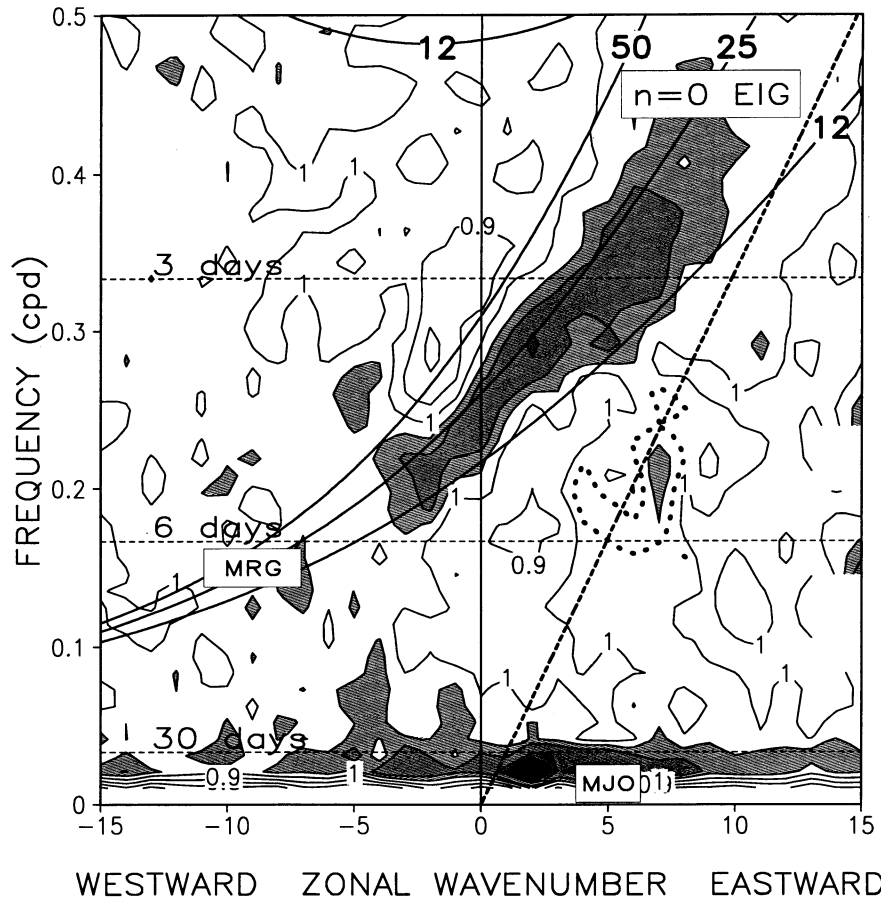
Fig. 1. Zonal wavenumber-frequency diagram of (a) antisymmetric (b) symmetric OLR spectral power divided by a background constructed by the revised method. Superimposed are the dispersion curves for the first even (a) odd (b) meridional mode for equivalent depths of 12, 25, and 50 m. The 25 m dispersion curve for the Kelvin waves is drawn in (a) as a dashed line and that for the mixed Rossby-gravity waves is drawn in (b) as a dashed curve. The dotted contour line surrounding the $F0.22E6-7$ region in (a) has a value of 1.05.

Fig. 2. Same as Fig. 1 but the background is constructed with the WK method.

Fig. 3. Same as Fig. 1 but only JJA data have been used.

Fig. 4. Same as Fig. 1 but only DJA data have been used.

(a) ANTI-SYMMETRIC: OLR power summed over 15°N–15°S/Background



(b) SYMMETRIC: OLR Power summed over 15°N – 15°S/Background

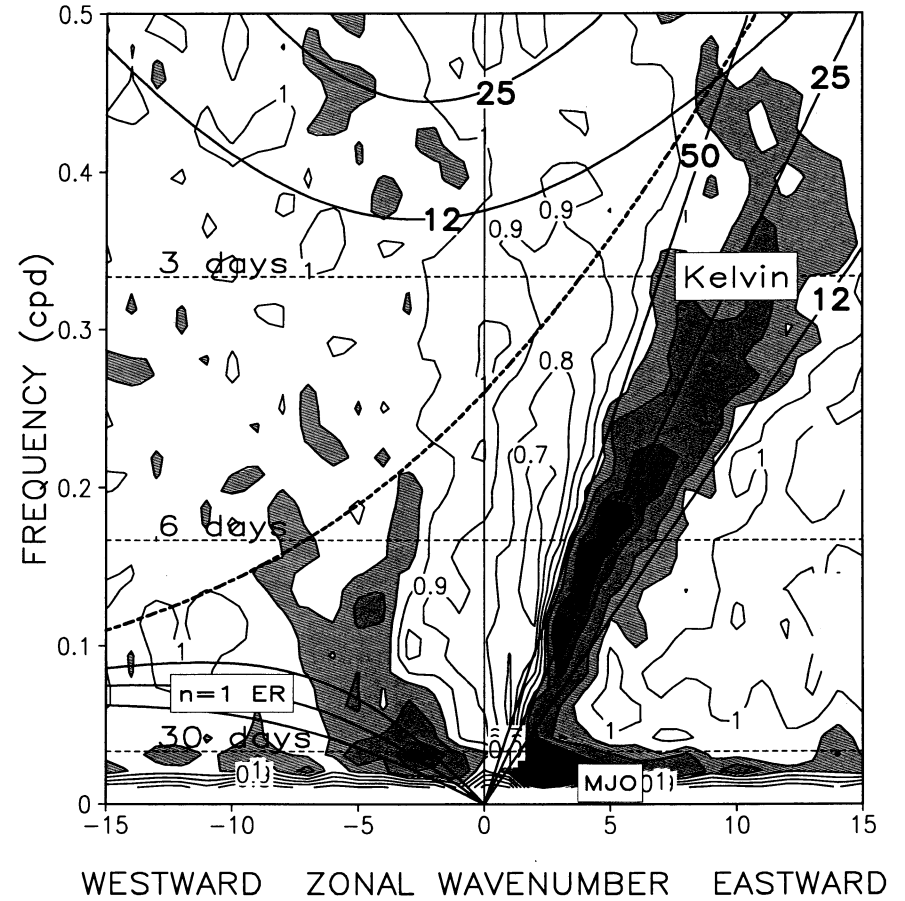
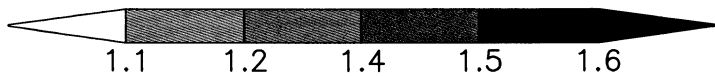
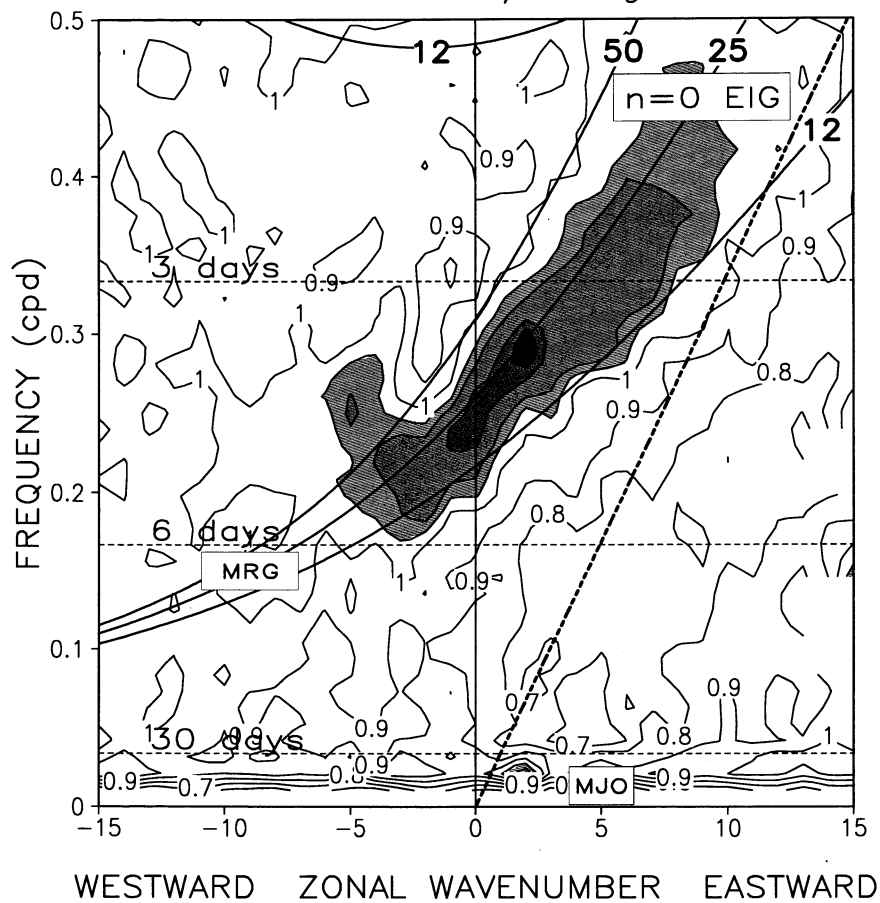


Fig. 1. Zonal wavenumber-frequency diagram of (a) antisymmetric (b) symmetric OLR spectral power divided by a background constructed by the revised method. Superimposed are the dispersion curves for the first even (a) odd (b) meridional mode for equivalent depths of 12, 25, and 50 m. The 25 m dispersion curve for the Kelvin waves is drawn in (a) as a dashed line and that for the mixed Rossby-gravity waves is drawn in (b) as a dashed curve. The dotted contour line surrounding the F0.22E6-7 region in (a) has a value of 1.05.

(a) ANTI-SYMMETRIC: OLR power summed over 15°N–15°S/Background



(b) SYMMETRIC: OLR Power summed over 15°N – 15°S/Background

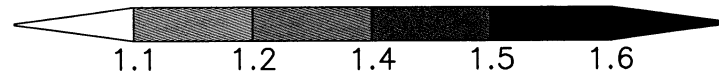
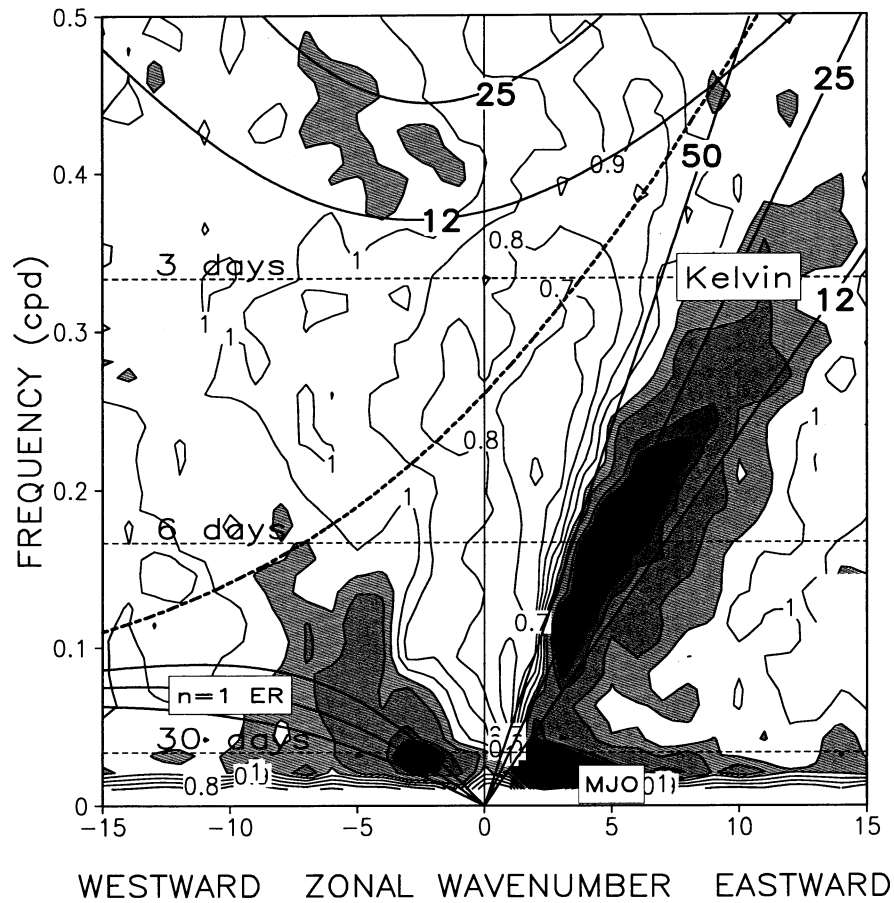
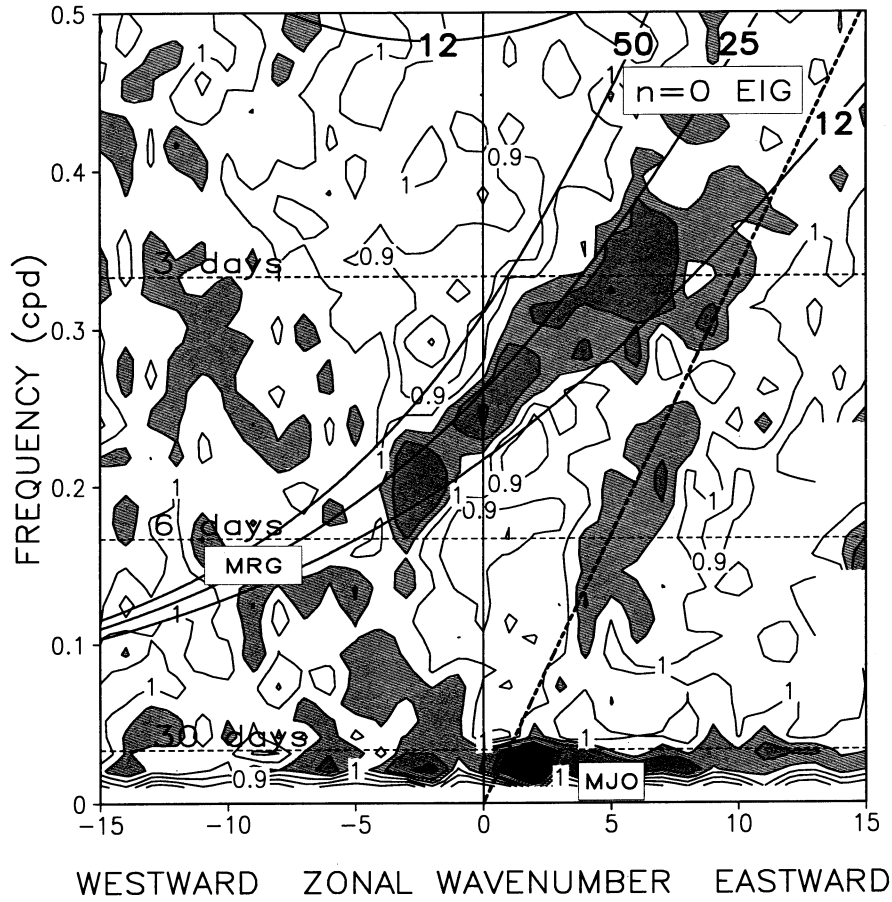


Fig. 2. Same as Fig. 1 but the background is constructed with the WK method.

(a) ANTI-SYMMETRIC: OLR power summed over 15°N–15°S/Background(JJA)



(b) SYMMETRIC: OLR Power summed over 15°N – 15°S/Background(JJA)

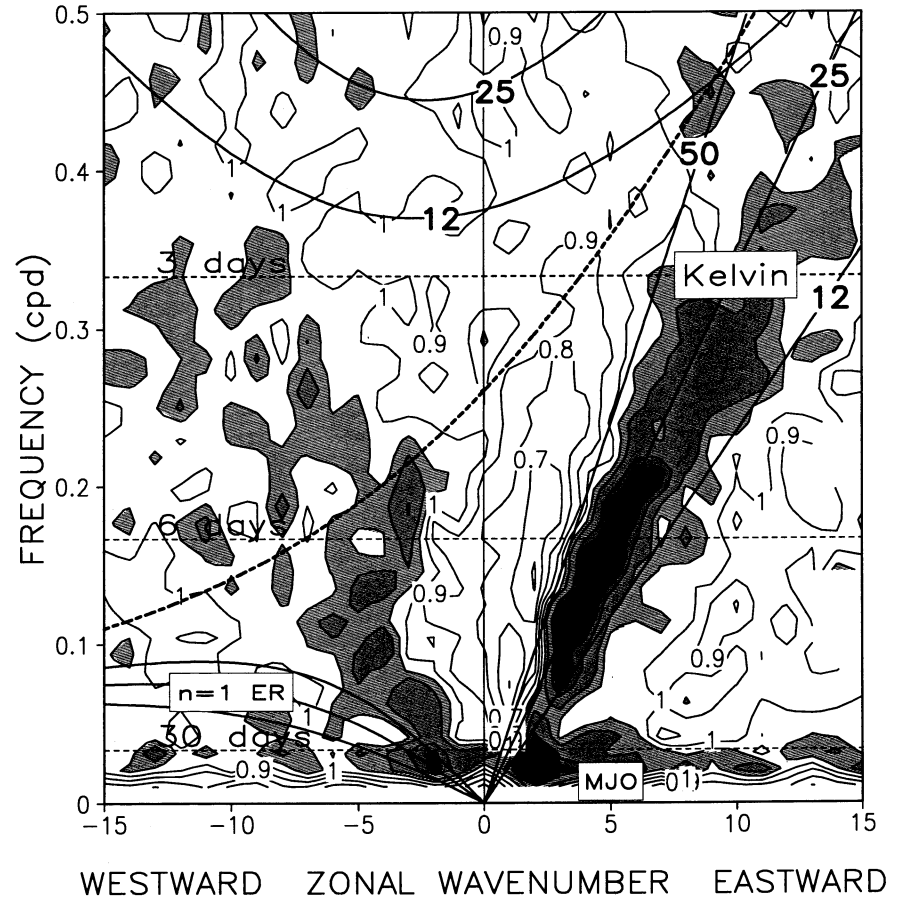
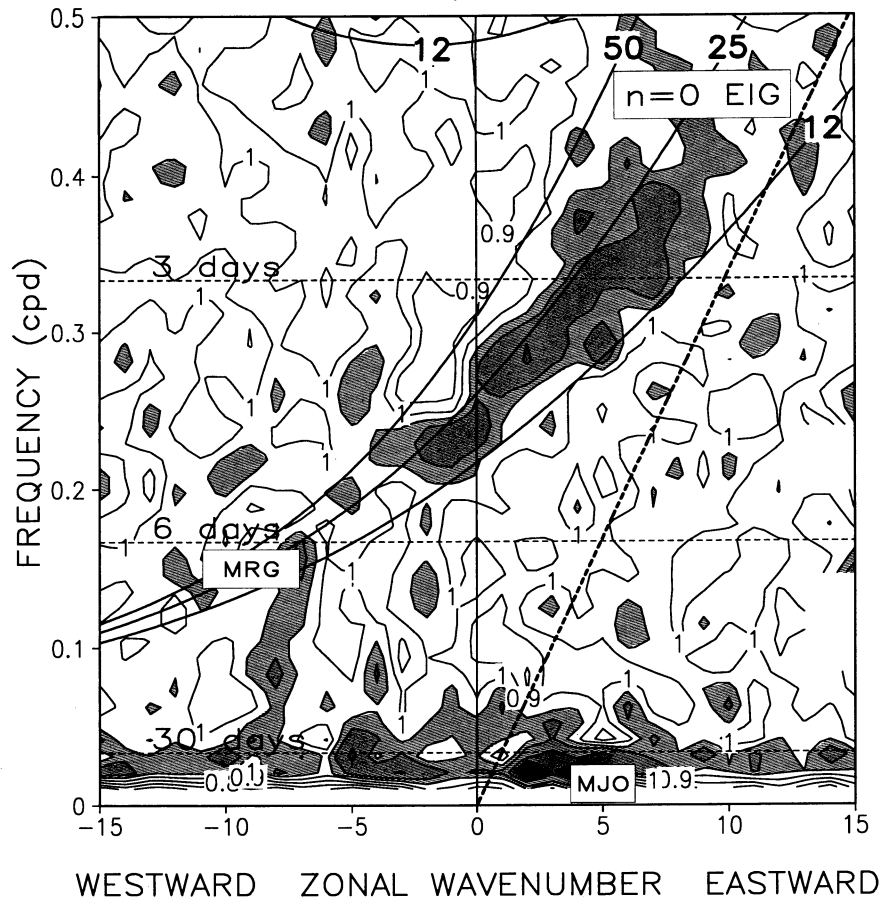


Fig. 3. Same as Fig. 1 but only JJA data have been used.

(a) ANTI-SYMMETRIC: OLR power summed over 15°N–15°S/Background(DJF)



(b) SYMMETRIC: OLR Power summed over 15°N – 15°S/Background(DJF)

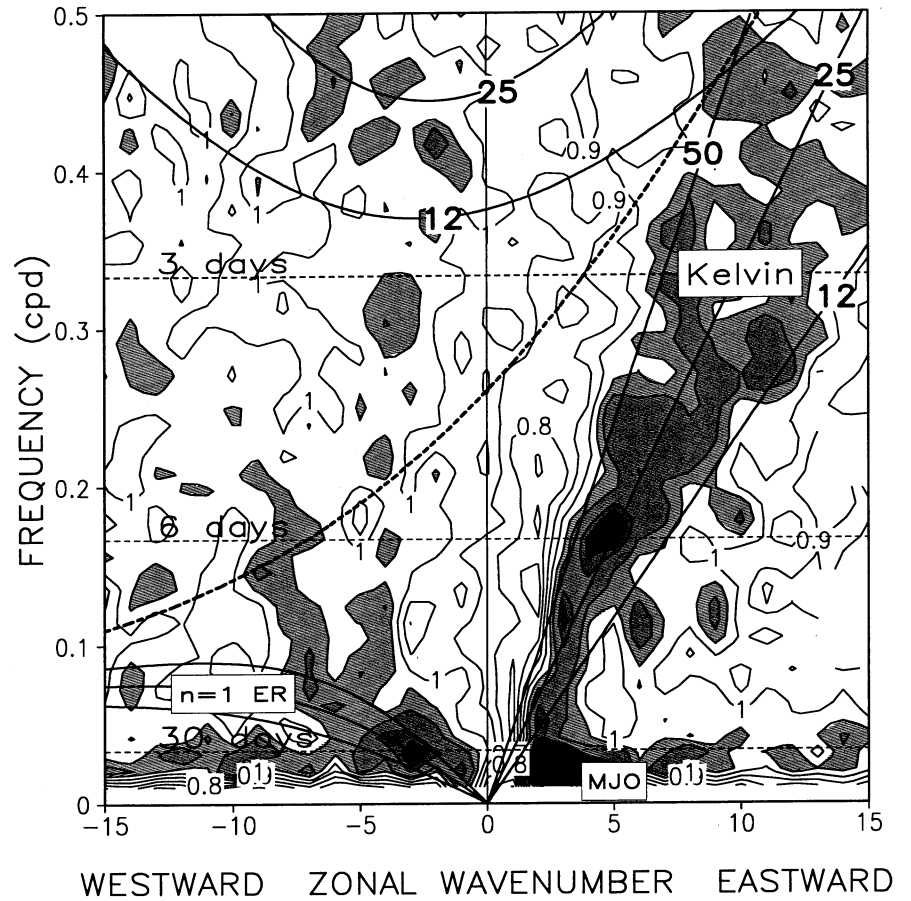


Fig. 4. Same as Fig. 1 but only DJA data have been used.